

Quadratic phase matching in nonlinear plasmonic nanoscale waveguides

Arthur R. Davoyan, Ilya V. Shadrivov, and Yuri S. Kivshar

Nonlinear Physics Center, Research School of Physics and Engineering, Australian National University, Canberra ACT 0200, Australia

ard124@physics.anu.edu.au

Abstract: We analyze phase matching in metal-dielectric nonlinear structures which support highly localized plasmon polariton modes. We reveal that quadratic phase matching between the plasmon modes of different symmetries becomes possible in planar waveguide geometries. We discuss the example of a nonlinear LiNbO₃ waveguide sandwiched between two silver plates, and demonstrate that second-harmonic generation can be achieved for interacting plasmonic modes.

© 2009 Optical Society of America

OCIS codes: (190.4350) Nonlinear optics at surfaces; (240.6680) Surface plasmons

References and links

1. A.D. Boardman, L. Pavlov, and S. Tanev, Eds., *Advanced Photonics with Second-order Optically Nonlinear Processes* (Kluwer Academic, Dordrecht, The Netherlands, 1998).
2. R.W. Boyd, *Nonlinear Optics* (Elsevier Science, USA 2003).
3. A. Di Falco, C. Conti, and G. Assanto "Quadratic phase matching in slot waveguides," *Opt. Lett.* **31**, 3146-3148 (2006).
4. H. Ishikawa and T. Kondo "Birefringent Phase matching in thin rectangular high-index-contrast waveguides," *Appl. Phys. Express* **2**, 042202 (2009).
5. S.A. Maier, *Plasmonics: Fundamentals and Applications* (Springer-Verlag, Berlin 2007).
6. E.N. Economou, "Surface plasmons in thin films," *Phys. Rev.* **182**, 539-554 (1969).
7. J.J. Burke, G.I. Stegeman, and T. Tamir, "Surface-polariton-like waves guided by thin, lossy metal films," *Phys. Rev. B* **33**, 5186-5201 (1986).
8. B. Prade, J.Y. Vinet, and A. Mysyrowicz, "Guided optical waves in planar heterostructures with negative dielectric constant," *Phys. Rev. B* **44**, 13556-13572 (1991).
9. J.A. Dionne, L.A. Sweatlock, H.A. Atwater, and A. Polman, "Plasmon slot waveguides: Towards chip-scale propagation with subwavelength-scale localization," *Phys. Rev. B* **73**, 035407 (2006).
10. Y. Satuby and M. Orenstein, "Surface plasmon polariton waveguides: From multimode stripe to a slot geometry," *Appl. Phys. Lett.* **90**, 251104 (2007).
11. N.-N. Feng and L. Dal Negro, "Plasmon mode transformation in modulated-index metal-dielectric slot waveguides," *Opt. Lett.* **32**, 3086-3088 (2007).
12. P. Neutens, P. Van Dorpe, I. De Vlaminc, L. Lagae, and G. Borghs, "Electrical detection of confined gap plasmons in metalinsulatormetal waveguides," *Nature Photon.* **3**, 283-286 (2009).
13. J.C. Quail and H.J. Simon "Second-harmonic generation with phase-matched long-range and short range surface plasmon polaritons," *J. Appl. Phys.* **56**, 2589-2591 (1984)
14. G.I. Stegeman, J.J. Burke, and D.G. Hall "Nonlinear optics of long range surface plasmons," *Appl. Phys. Lett.* **41**, 906-908 (1982).
15. P.B. Johnson and R.W. Christy, "Optical constants of noble metals," *Phys. Rev. B* **6**, 4370-4379 (1972).
16. R.S. Weis and T.K. Gaylord, "Lithium Niobate: Summary of physical properties and crystal structure," *Appl. Phys. A* **37**, 191-203 (1985).
17. A.R. Davoyan, I.V. Shadrivov, and Yu.S. Kivshar, "Nonlinear plasmonic slot waveguides," *Opt. Express* **16**, 21209-21214 (2008).
18. A.R. Davoyan, I.V. Shadrivov, and Yu.S. Kivshar, "Nonlinear plasmonic slot waveguides: erratum," *Opt. Express* **17**, 4833 (2009).

1. Introduction

The study of optical frequency conversion and second-harmonic generation is one of the key topics of nonlinear optics with already demonstrated numerous applications. The frequency doubling was studied in various systems and under many different conditions (for a general overview see, e.g., Refs. [1, 2]). The main requirement for many of such parametric processes is phase matching which should be satisfied either in bulk or waveguiding structures. Several approaches to achieve efficient phase matching in crystals and waveguides have been suggested and demonstrated, including the use of birefringence and quasi-phase matching. Many of such methods have physical limitations, for example, birefringence often does not provide collinear phase matching, whereas quasi-phase matching at nanoscales is limited by fabrication challenges. One of the recently discussed novel possibilities of phase matching is based on tailoring the mode dispersion in nanoscale waveguides [3, 4]. In particular, it was shown that collinear phase matching between TM and TE modes becomes possible for the subwavelength dimensions of a slot waveguide [3] or a high-index guiding slab [4]. However, since a change of polarization is implemented, the effective mode size can not be less than a half of the wavelength.

Plasmonic waveguides offer many novel opportunities for subwavelength confinement and other applications, including sensing, imaging, and signal processing. Optical waveguides based on plasmon polaritons are at the core of research in nanophotonics, and different types of metal-dielectric waveguides have been suggested theoretically and demonstrated experimentally (see, e.g., Refs. [5–12] to cite a few). The study of nonlinear optics in plasmonic systems is of a great interest with many potential applications. Until now, many studies have demonstrated the excitation of plasmons through the second-order optical processes [13, 14].

This paper aims to apply a novel phase-matching scheme [3, 4] to the case of plasmonic waveguiding and to study the possibility of plasmon-to-plasmon conversion in planar metal-dielectric nonlinear waveguides. We demonstrate that phase matching condition between plasmons can be achieved in nanoscale plasmonic waveguides where the waveguide width becomes smaller than a certain threshold value. We analyze the second-harmonic generation due to phase matching and parametric conversion between the plasmonic modes of different symmetries which cannot be achieved in dielectric waveguides.

2. Slot waveguides

For plasmonic waveguiding, two major planar geometries have been suggested: metal-dielectric-metal structures (slot waveguide), and thin metallic films embedded into dielectric media. Here, we discuss the case of a nonlinear plasmonic slot waveguide.

We consider an anisotropic dielectric slab with the thickness a sandwiched between two semi-infinite metallic slabs, see Fig. 1(a). For this structure, we present the dielectric constant in the form,

$$\varepsilon = \begin{cases} \varepsilon_m(\omega), & \text{in metallic layers,} \\ \begin{pmatrix} \varepsilon_x & 0 & 0 \\ 0 & \varepsilon_y & 0 \\ 0 & 0 & \varepsilon_z \end{pmatrix}, & \text{in anisotropic dielectric slab.} \end{cases}$$

We note that dielectric constant of metal varies with frequency, and it can be described by the Drude-Lorentz model, $\varepsilon_m(\omega) \simeq \Sigma[\delta_i/(\omega^2 - \omega_i^2 - 2\gamma_i\omega)]$, that agrees well with the experimental data [5, 15] in wide frequency range when up to seven Lorentz poles are taken into account.

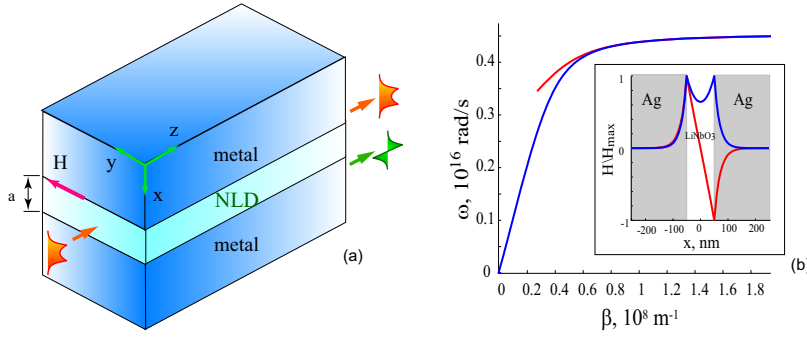


Fig. 1. (a) Schematic of a slot waveguide of the width a . (b) Dispersion relation for a 100nm thick lithium-niobate waveguide placed between two silver plates. Blue curve - symmetric branch, red curve - antisymmetric branch. The inset shows a typical profile of the magnetic field in the structure.

Earlier studies of plasmonic waveguides (see, e.g., Refs. [6–8]) demonstrated that in the linear regime only TM waves can propagate in such structures in subwavelength regime, i.e. the magnetic vector is in the interface plane, $\mathbf{H} = (0, H_y, 0)$, see Fig. 1(a). Thus the electric field is described by two components: $\mathbf{E} = (E_x, 0, E_z)$, which in the nonlinear case leads to complicated interaction between them. Considering that the structure is invariant in the y axis and plasmons propagate in the slot along the z direction with the plasmon propagation constant β , and applying the corresponding boundary conditions, we obtain [8]:

$$\tanh\left(\frac{\kappa_d a}{2}\right) = - \begin{cases} \begin{pmatrix} \varepsilon_z \kappa_m \\ \varepsilon_m \kappa_d \end{pmatrix}, & \text{symmetric mode,} \\ \begin{pmatrix} \varepsilon_m \kappa_d \\ \varepsilon_z \kappa_m \end{pmatrix}, & \text{antisymmetric mode,} \end{cases} \quad (1)$$

where $\kappa_d = [\beta^2(\varepsilon_z/\varepsilon_x) - \varepsilon_z]^{1/2}$ and $\kappa_m = (\beta^2 - \varepsilon_m)^{1/2}$. Note that while discussing the dispersion relations and the possibility of phase-matching conditions in plasmonic structures we do not take losses into account, however we will consider them below for calculating the resulting conversion efficiency.

For small widths of the slot waveguide, the dispersion relation splits into two branches: lower (symmetric) branch and upper (antisymmetric) branch. For relatively large widths of the slot waveguide, both branches merge into one, corresponding to single interface plasmon polariton mode [8].

To be more specific, we consider silver for the metal (as the material extensively used for plasmonic applications due to its relatively low losses), and lithium niobate LiNbO_3 as a nonlinear dielectric (also widely used for second-order optical parametric processes). Lithium niobate is a uniaxial crystal with trigonal symmetry (having three nonzero components of the second-order susceptibility tensor in our geometry) [16], and for nanoscale fabrications it is convenient to orientate the crystalline axis along the propagation direction since this direction is mechanically most stable [16]. The dielectric constants of LiNbO_3 are $\varepsilon_x = 5.52$ and $\varepsilon_z = 5.06$.

In Fig. 1(b), we plot the linear dispersion relations (1) for slot waveguide with 100nm width. The dispersion curves are presented by lower (symmetric) and upper (antisymmetric) branches. Typical magnetic field profiles for both branches are presented in the inset to Fig. 1(b).

To reveal the possibility of plasmonic frequency conversion in such a structure, first we should analyze the phase matching conditions. We calculate the plasmonic guide indices for the fundamental frequency (FF) and second harmonic (SH) depending on the slot width, Fig. 2. In Fig. 2(a) we plot the guide index vs. the slot width for free space FF wavelength $\lambda_0 =$

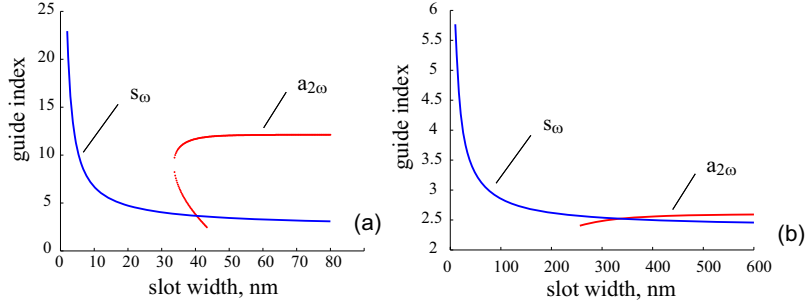


Fig. 2. Plasmonic guide index versus the slot width for different FF wavelengths: (a) $\lambda_0 = 840\text{nm}$ ($\epsilon_m = -23.4 + i1.628$) and (b) $\lambda_0 = 1550\text{nm}$ ($\epsilon_m = -103.2 + i8.11$). Notations "s" and "a" stand for the symmetric and antisymmetric modes, respectively, and the indices ω and 2ω correspond to the fundamental and second harmonics, respectively.

840nm. For this case, we observe that the exact phase matching between the symmetric and antisymmetric modes becomes possible for a slot of 40nm. Moreover, in this case the phase matching occurs between the *forward symmetric* and *backward antisymmetric* mode [17, 18]. For the fundamental frequency at $\lambda_0 = 1550\text{nm}$, the linear phase matching occurs for the slot width $a \simeq 320\text{nm}$, and in this case both FF and SH are forward waves. However, the phase matching is not a sufficient condition, and the mode interactions and overlaps should be studied at the next step, especially when the parametric interaction involves the modes of different symmetries.

Now we calculate the dependence of the waveguide thickness required for the exact phase matching on the free-space wavelength of the fundamental wave, and plot it in Fig. 3(a). We note that the dispersion characteristics can be tuned for slot waveguides having finite y dimensions. Introducing the y dimension, we can obtain an extra degree of freedom to satisfy phase matching conditions and reach optimum efficiency [3].

As the next step, we calculate the components of the nonlinear polarization responsible for the second-harmonic generation. We assume that during the parametric interaction the surface plasmons remain TM polarized, i.e $\mathbf{E} = (E_x, 0, E_z)$, and thus the nonlinear polarization has two components $\mathbf{P} = (P_x, 0, P_z)$. Since the susceptibility tensor of LiNbO₃ has three nonzero components d_{31} , d_{33} and d_{15} in our geometry, the nonlinear polarization P at fundamental frequency and second harmonic for planar plasmonic structure can be presented as follows [1]:

$$\begin{aligned} P_x^\omega &= d_{15} [(E_x^\omega)^* E_z^{2\omega} + (E_z^\omega)^* E_x^{2\omega}], & P_z^\omega &= d_{31} (E_x^\omega)^* E_x^{2\omega} + d_{33} (E_z^\omega)^* E_z^{2\omega}, \\ P_x^{2\omega} &= d_{15} E_x^\omega E_z^\omega, & P_z^{2\omega} &= \frac{1}{2} [d_{31} (E_x^\omega)^2 + d_{33} (E_z^\omega)^2]. \end{aligned} \quad (2)$$

Here the superscripts ω and 2ω correspond to the fundamental and second-harmonic waves.

To illustrate the interaction between different field components in Eq. (2), in Fig. 4 we show the mode profiles at the fundamental frequency and second-harmonics, and study the effect of the mode interaction. According to this diagram, for the symmetric FF mode, the electric field component E_x^ω is symmetric, and E_z^ω is antisymmetric, whereas for the second-harmonic field the symmetries are reversed, namely $E_x^{2\omega}$ is antisymmetric, and $E_z^{2\omega}$ is symmetric. Corresponding polarization components are shown schematically in Fig. 4.

To describe the interaction of the mode at the fundamental frequency with the mode of the second harmonics, we follow the approach suggested in Ref. [19], and derive the equations for

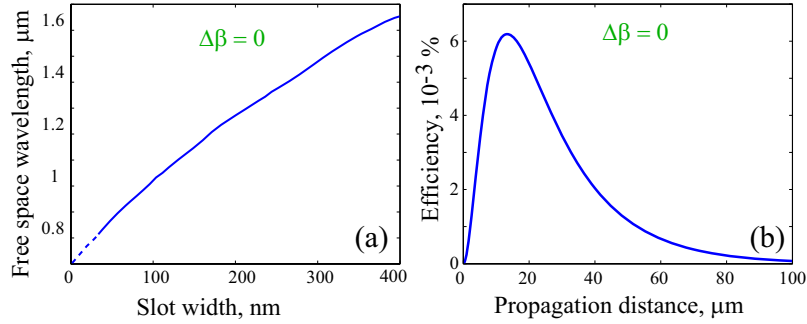


Fig. 3. (a) Free-space wavelength vs the slot width in the case of the exact phase matching in a plasmonic slot waveguide. (b) Efficiency of the second-harmonic generation as a function of the propagation distance (or the device length).

the slowly varying mode amplitudes:

$$\begin{aligned}\frac{dA_1}{dz} &= -\alpha_1 A_1 + i\Gamma_1 A_1^* A_2 e^{i\Delta\beta z}, \\ \frac{dA_2}{dz} &= -\alpha_2 A_2 + i\Gamma_2 A_1^2 e^{-i\Delta\beta z}\end{aligned}\quad (3)$$

where A_m are the amplitudes of FF and SH modes defined through the expression

$$\mathbf{E}_m = A_m(z)[\mathbf{x}E_{x0}^{(m)}(x) + \mathbf{z}E_{z0}^{(m)}(x)]e^{i\beta_m z - im\omega t},$$

where $E_{x0,z0}^{(m)}$ are the profiles of the linear modes in the guiding structure at the corresponding frequencies, $m = 1, 2$; $\Delta\beta = \beta_2 - 2\beta_1$ is the phase mismatch, and

$$\begin{aligned}\alpha_m &= m \frac{\int \varepsilon''(m\omega) |\mathbf{E}_0^{(m)}|^2 dx}{2 \int E_{x0}^{(m)} H_{y0}^{(m)} dx}, \\ \Gamma_m &= 2\pi m \frac{\int [P_{x0}^{(m)} E_{x0}^{(m)} + P_{z0}^{(m)} E_{z0}^{(m)}] dx}{\int E_{x0}^{(m)} H_{y0}^{(m)} dx},\end{aligned}$$

where ε'' is the imaginary part of the dielectric permittivity, and $\mathbf{P}_0^{(m)}$ are the corresponding polarizations obtained by substituting linear modes into Eq. (2).

In a sharp contrast to dielectric waveguides, the conversion between the FF symmetric mode and SH antisymmetric mode becomes possible for plasmonic waveguides, as shown in Fig. 4. Within the undepleted pump approximation, when the amplitude at fundamental frequency is not affected by nonlinearity, and also for the exact phase matching, $\Delta\beta = 0$, we obtain

$$\begin{aligned}A_1 &= A_1(0) \exp(-\alpha_1 z), \\ A_2 &= \frac{i\Gamma_2 A_1(0)^2}{(\alpha_2 - 2\alpha_1)} [\exp(-2\alpha_1 z) - \exp(-\alpha_2 z)]\end{aligned}$$

Now we introduce the normalized conversion efficiency as follows,

$$\eta = \frac{\text{Power}(2\omega)}{\text{Power}(\omega)} = \frac{|A_2|^2 \int E_{x0}^{(2)} H_{y0}^{(2)} dx}{|A_1|^2 \int E_{x0}^{(1)} H_{y0}^{(1)} dx}.$$

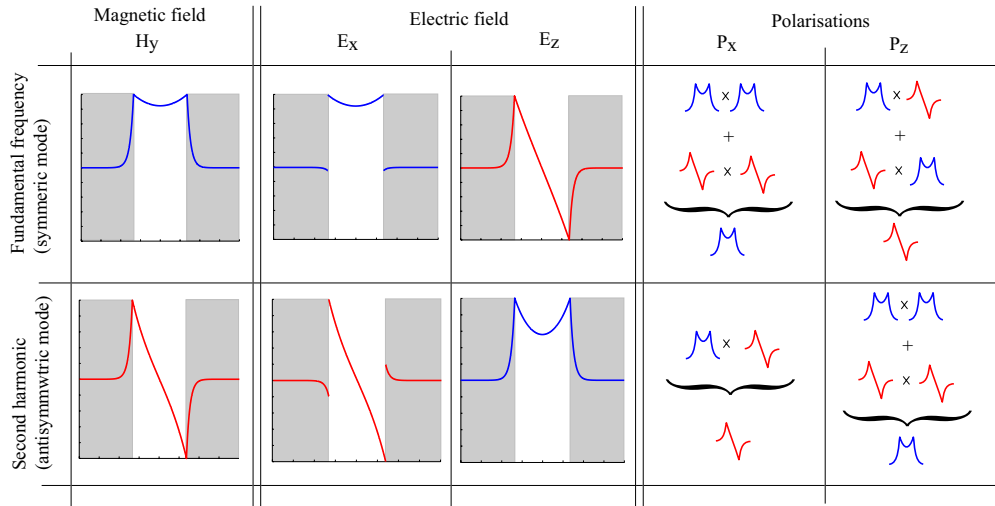


Fig. 4. Structure of modes for the phase-matching in a plasmonic slot waveguide. The upper row corresponds to the field components of a symmetric mode at the fundamental frequency, lower row - an antisymmetric mode of the second-harmonic field.

Dependence of the conversion efficiency on the propagation distance (or the device length) in the case of the exact phase matching is shown in Fig. 3(b). The FF pump power is 10 MW/m, and the free-space wavelength is $\lambda = 1550\text{nm}$. The efficiency curve displays a characteristic interplay between the SH generation and losses, which manifests itself a maximum of the conversion efficiency at $\sim 15\mu\text{m}$.

We note that equations similar to Eq. (3) can also be derived for the second-order nonlinear processes with plasmons guided by a thin metallic film embedded into nonlinear dielectric media. We have analyzed the phase-matching conditions for this case as well, and have found that, in contrast to the slot waveguide, the lower branch of the dispersion curves describes an antisymmetric mode, whereas the upper branch describes a symmetric mode [8]. We have calculated the guiding indices for various wavelengths and revealed that the phase matching becomes possible between an antisymmetric FF mode and a symmetric SH mode.

3. Conclusions

We have analyzed parametric processes in nonlinear plasmonic waveguides and demonstrated that quadratic phase matching can be satisfied for the guided plasmonic modes of different symmetries in nanoscale slot waveguides. Our analysis of the mode coupling has revealed that phase-matched second-harmonic generation can be achieved for a wide range of frequencies of the fundamental wave by an appropriate choice of the slot width. We believe that the current technology would allow fabrication of such thin nanoscale nonlinear waveguides with the subsequent applications to ultra-compact plasmonic devices based on the parametric processes.

Acknowledgements

The authors acknowledge a support of the Australian Research Council, and enlightened discussions with D. Gramotnev and N. Zheludev.